International Journal of Bridge Engineering (IJBE), Vol. 9, No. 3, (2021), pp. 51-84

THE INVESTIGATION OF THE EFFECTS OF USING ENERGY DISSIPATION EQUIPMENT IN SEISMIC RETROFITTING AN EXIST HIGHWAY RC BRIDGE SUBJECTED TO FAR-FAULT EARTHQUAKES

Saman Mansouri

Department of Civil Engineering, Dezfoul Branch, Islamic Azad University, Dezfoul, Iran.
e-mail: samanmansouri@iaud.ac.ir

ABSTRACT: In this paper, the strategies for seismic retrofit of the bridge located on Dogaz's highway interchange with the Tehran-Karaj freeway have been discussed. The conventional neoprene has been used between decks with abutments and cap beams of this bridge. Since the neoprene bearings do not have the high capacity of energy dissipation due to the earthquake, therefore, to this end, appropriate strategies for seismic retrofitting the bridge should be adopted. The method of the study is, first, the alternative effects of elastomeric bearings (the second model), lead rubber bearing (the third model) and friction pendulum bearing (the forth model) instead of neoprene have been evaluated and compared in three separate models and then when the deck with rigid connection is on the cap beams and abutments (the first model) have been evaluated in another model. The results of the Eigen vector analysis indicates that model the use of elastomeric bearings (EB), lead rubber bearing (LRB) and friction pendulum bearing (FPB) makes the most of the energy caused by vibration dissipate in modes where the structures have simple deformation compared with first model and also using the discussed seismic bearing makes to prevent the complicated warping of the bridges slightly than the first model. The results of non-linear time history analysis indicates that the displacement of deck, cap beams and abutment is equal in the first model and its value is very low and this seismic behavior makes considerable increase of shear base force in integrated bridge in comparison with isolated ones. While enjoying discussed seismic bearings make deck slide on seismic bearings under the effect of earthquake that this seismic behavior leads to increase the absorption and dissipation of energy in the isolated structure than integrated structure.

KEYWORDS: Seismic retrofit, Existing bridge, Lead Rubber Bearing, Elastomeric Bearings, Friction Pendulum Bearing.

1 INTRODUCTION

The review of the earthquakes in recent decades has indicated that a large number of bridges are damaged significantly by earthquakes. Regarding the strategic role of the bridges in the transportation system, bridges closure can lead to different damages. Therefore, the study of the seismic response of bridges from different aspects is of particular importance (Mansouri, 2020). One of the most important solutions to prevent of the seismic damages of bridges is their seismic retrofit using seismic bearings.

Recently, many different studies have been conducted on the effects of the using energy dissipation equipment in seismic retrofitting structures, including Parvari et al. (2018); Li and Shi (2019); Zheng (2020); Ju et al. (2020). In addition, Qiang et al. (2009) showed that many highway bridges were severely damaged or completely collapsed during the 2008 Wenchuan earthquake. A field investigation was carried out in the strongly affected areas and over 320 bridges were examined. The most common damage included shear-flexural failure of the pier columns, expansion joint failure, shear key failure, and girder sliding in the transversal or longitudinal directions due to weak connections between girder and bearings. Lessons learned from the earthquake were described and recommendations related to the design of curved and skewed bridges, design of bearings and devices to prevent girder collapse, and ductility of bridge piers were presented. Kaheh (2011) showed that conventional neoprene did not have a high ability to dissipate energy caused by earthquakes in the bridges. Caterino et al. (2014) investigated the damage analysis and seismic retrofit of a continuous pre-stressed RC bridge. The results of their analysis indicated that the structural performance could be enhanced by only modifying the support devices. The primary structural components were not required to be involved in the retrofitting process. Using the modern seismic code, the upgrading of the viaduct performance was obtained by replacing the old bearing devices on the piers and existing viscous dampers connected abutments to the deck with new modernised ones. Mansouri et al. (2013-2017) investigated that the effect of using the energy dissipation equipment on bridges and buildings. They showed that using the seismic bearings and dampers could reduce the seismic response of structures. Avossa et al. (2018) examined that the seismic retrofit of a pre-stressed concrete girder bridge with friction pendulum devices. Furthermore, to assess the impact of the FPD nonlinear behavior on the bridge seismic response, a device model that reproduces the variation of the normal force and friction coefficient, the bidirectional coupling, and the large deformation effects during nonlinear dynamic analyses was used. Finally, the paper examines the effects of the FPD modelling parameters on the behavior of the retrofitted bridge and assesses its seismic response with the results pointing out the efficiency of the adopted seismic retrofit solution. Ma et al. (2020) examined that the dynamic response analysis of story-adding structure with isolation technique subjected to near-fault

pulse-like ground motions. In their paper, a story-adding seismic structure, a base-isolated structure, and a story-adding isolated structure were simulated by using numerical simulation methods. The dynamic response characteristics of the three structures under near-fault pulse-like ground motions were analysed and compared with the far-fault ground motions. The results showed that using the base isolation could significantly extend the period of the main structure and reduce the seismic response on the upper structure. The inter-story drift ratio, inter-story shear force, and the story acceleration of all three structures under near-field pulse-like ground motions were all larger than that of far-field earthquakes. Both base-isolated structure and story-adding isolated structure showed excellent damping performance. Besides, the damping properties of the base-isolated structure were better than the story-adding isolated structure. Li et al. (2020) investigated that the energy response analysis of continuous beam bridges with friction pendulum bearing by multi-hazard source excitations. The influence of the friction coefficient and isolation period of the FPB on the energy response of isolated bridge was then investigated under multi-hazard source excitations with different dominant periods and durations. The variations of structural response energy, sliding displacement, energy dissipation ratio, and acceleration of the isolated bridges were plotted. The results of analytical modelling and finite element simulation showed good agreement. In addition, there exist particular values of the friction coefficient and isolation period of FPB, for which the structural response energy of the isolated bridges attained the minimum value. The optimal parameters of FPB were greatly influenced by seismic waves, and the friction coefficient of FPB should be increased with the increase of seismic fortification intensity. In addition, the energy dissipation capacity of FPB used in isolated bridge was excellent. Ma and et al. (2021) examined the dynamic response of story-adding structure with isolation technique subjected to near-fault ground motions. The results showed that using the base isolation could significantly extend the period of the main structure and reduce the seismic response on the upper structure. The inter-story drift ratio, inter-story shear force, and the story acceleration of all three structures under near-field pulse-like ground motions were all larger than that of far-field earthquakes. Besides, both base-isolated structures and story-isolated structures showed good damping effect. The base-isolated structures showed better seismic performance than the adding-story-isolated structures. Besides, many valuable studies on the effect of different characteristics of earthquakes on bridges in far-fault earthquakes have been conducted, including Mansouri (2020, 2021).

Although many studies have been conducted by researchers in recent years concerning the effects of using the energy dissipation equipment on the seismic response of the bridges, some of which were mentioned, a comprehensive study has not been done thus far to investigate the using different seismic bearings on an existing highway RC bridges subjected to far-fault earthquakes. Therefore, the effects of the using different seismic bearings on the seismic response of the RC

bridges subjected to far-fault earthquakes are investigated in this study, so that first, the considered bridge was modeled. Then, the Eigen vector analysis and the nonlinear time history analysis were used to evaluate the response of a RC bridge at different states with and without applying the effect of the using different seismic bearings.

2 THE STUDIED BRIDGE

A sixth-span existing RC bridge was investigated in this study. The length of lateral and middle spans was 12.6m and 18.5m, respectively. The width of the deck was 17m. The studied bridge was located at the non-level intersection of Dogaz highway with Tehran-Karaj freeway, which is shown in Fig. 1.

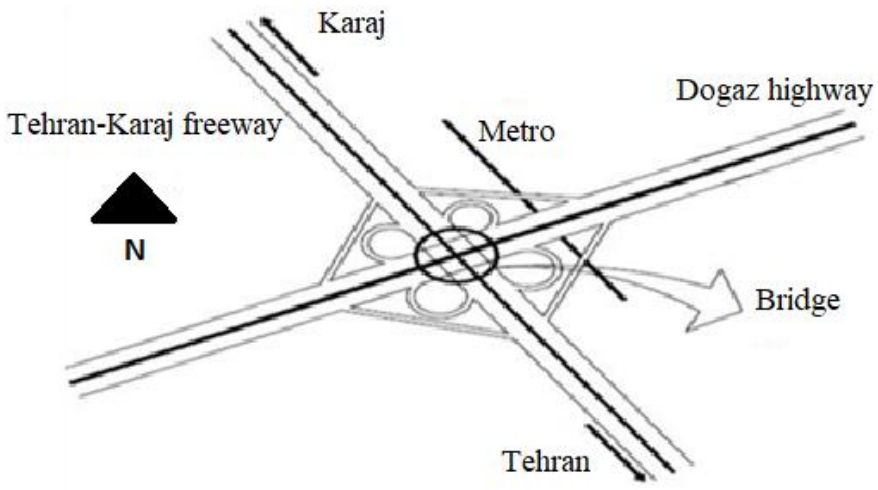

Figure 1a. The location of the bridge under study

Each of the five cap beams has four columns. The cross-section of columns was a circle with a diameter of 120cm and the cross-section of abutments were rectangular with a height of 130cm and a width of 190cm. Other specifications of the studied bridge are according to Figs. 1-b to 1-e.

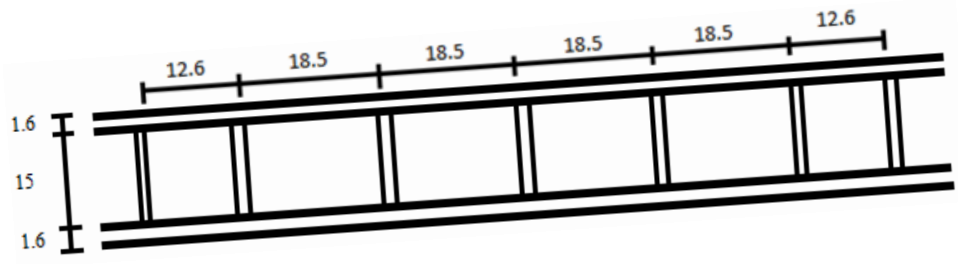

Figure 1b. Plan view

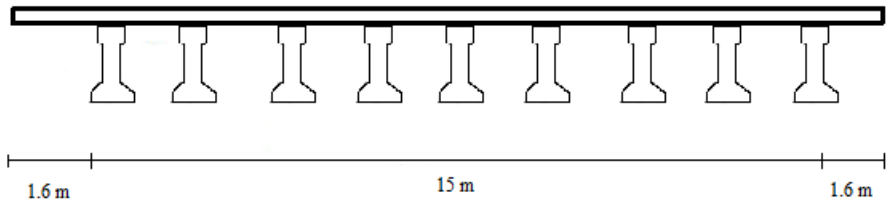

Figure 1c. Cross-section of deck

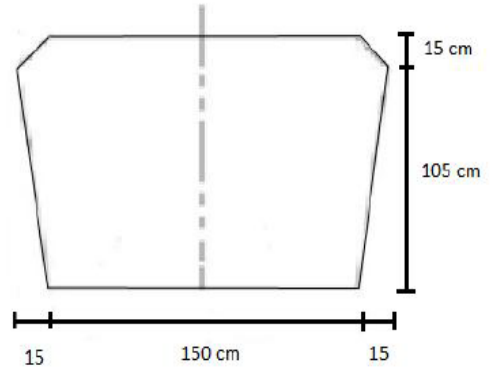

Figure 1d. Cross-section of bent

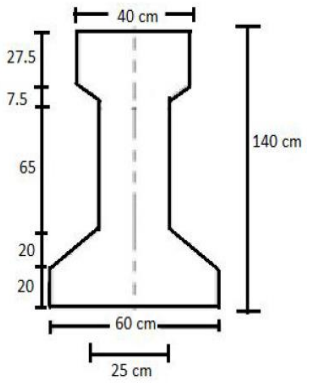

Figure 1e. Cross-section of beam

Figure 1. The studied bridge

The conventional neoprene is used between the deck with abutments and cap beams. The thickness of the deck slab is equal to 27.5cm.

3 ENERGY DISSIPATION EQUIPMENT

3.1 Elastomeric bearing (EB)

Elastomeric bearing is mostly made out of laminated rubber with more than one reinforcing steel sheets inside. Rubber is used as the major material for flexible bending rigidity and the steel sheets are inserted to reinforce the horizontal stiffness. A view and features of the elastomeric bearings are as shown in Figs. 2 to 4.

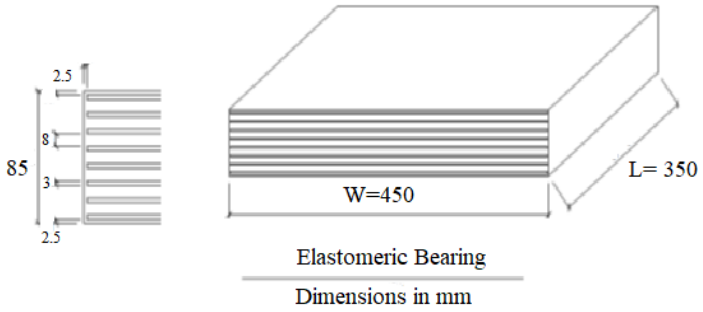

Figure 2. A view of elastomeric bearing (Akogul and Celik, 2008)

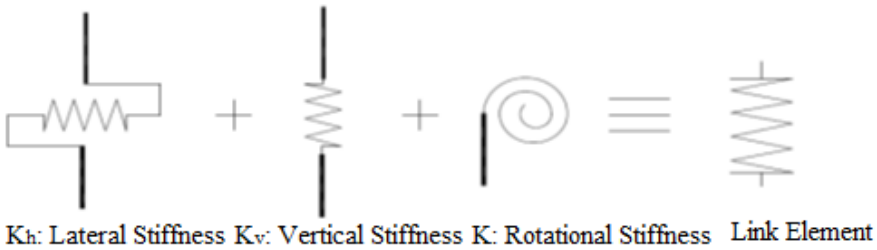

Figure 3. The link element (Akogul and Celik, 2008)

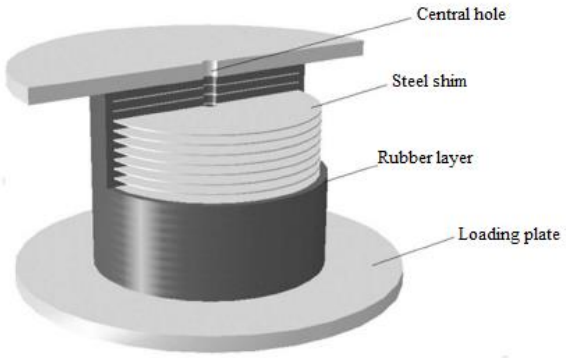

Figure 4. A view of detail of elastomeric bearing (Jabbareh et al. 2014)

Using the following information, EB can be modeled (Akogul and Celik, 2008):

$$K_H = k_{eff} = \frac{G_{eff}A}{H_r} = \frac{680 \times 0.1575}{0.061} = 1755KN/m$$

$$K_V = \frac{E_C A}{H} = \frac{617263 \times 0.1575}{0.085} = 1143752KN/m$$

$$K_\theta = \frac{EI}{H_r} = \frac{617263 \times 0.0016}{0.061} = 16270KNm/m$$

3.2 Lead rubber bearing (LRB)

Lead rubber bearing (LRB) is designed to improve the weakness of rubber bearing (RB or EB). RB has low damping and displays huge deformation for static loads. Therefore, LRB inserts a lead plug in RB, as shown in Fig. 5, to provide damping to response to earthquakes and to resist static loads. Because the lead plug inserted into the LRB is characterized by almost full elasto-plastic hysteresis loop, the rigidity of the bearing after the yielding of the lead is equal to that of RB, and the capacity of LRB can be determined by vertical load, random horizontal reaction, and scale of construction expansion. Generally, in the case of designing a LRB, the diameter of the lead plug that is determined by the coefficient of horizontal reaction and should be ideally small (Han et al. 2009). Fig. 5 shows a view of lead rubber bearing and Fig. 6 shows the using LRB in bridges.

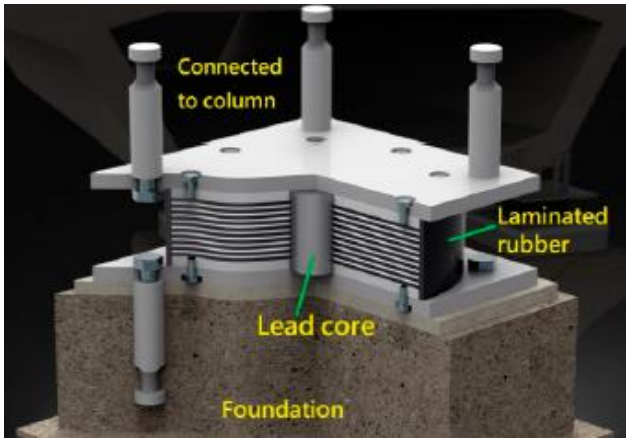

Figure 5. A view of lead rubber bearing (Ju et al. 2020)

Figure 6. The using LRB in bridges (Photo by Saman Mansouri)

LRB can be modeled with the following specifications (Torunbalci and Ozpalanlar, 2008):
Link element= Rubber Isolator
U1→ linear Effective Stiffness= 1500000 KN/M
U2=U3 → linear Effective Stiffness= 800 KN/M
U2=U3 → Nonlinear Stiffness=2500 KN/M
U2=U3 → Yield Strength= 80
U2=U3 → Post Yield Stiffness Ratio= 0.1

3.3 Friction pendulum bearing (FPB)

The FPB are normally installed between the superstructure and the substructure as shown in Fig. 7, with equal distribution of the weight of the superstructure on each FPB. Fig. 8 shows a view of theoretical hysteresis curve of the FPB. Fig. 9 shows a view of the friction pendulum bearing.

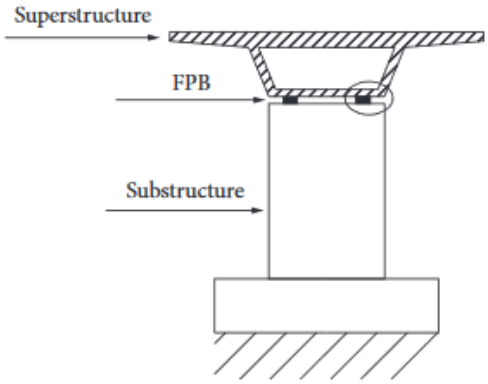

Figure 7. The isolated bridge with 2 FPBs in view of the axial direction of the bridge (Li et al. (2020))

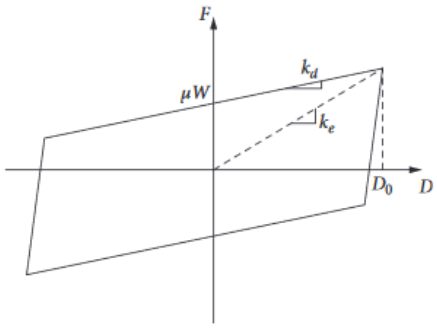

Figure 8. Bilinear hysteresis model (Li et al. (2020))

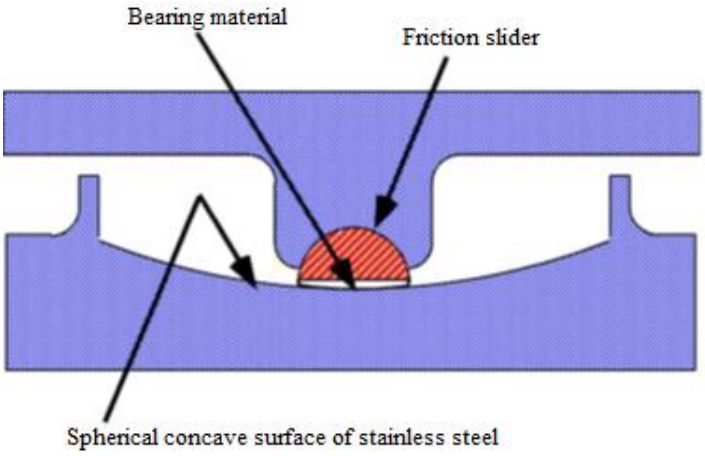

Figure 9. A view of the friction pendulum bearing (Okamura and Fujita, 2007)

FPB can be modeled with the following specifications (Torunbalci and Ozpalanlar, 2008):
Link element= Friction isolator
U1 → linear Effective Stiffness= 15000000 KN/M
U1 → Nonlinear Effective Stiffness= 15000000 KN/M
U2=U3 → linear Effective Stiffness= 750 KN/M
U2=U3 → Nonlinear Stiffness=15000 KN/M
U2=U3 → Friction Coefficient Slow= 0.03
U2=U3 → Friction Coefficient Slow= 0.05
U2=U3 → Rate Parameter= 40
U2=U3 → Radius of Sliding Surface= 2.23

4 THE STUDIED MODELS

The conventional neoprene (rubber bearings with high damping) has been used between decks with abutments and cap beams of this bridge. Since the neoprene bearings do not have the high capacity of energy dissipation due to the earthquake, therefore, to this end, appropriate strategies to seismic retrofit of the bridge should be adopted. The method of this study is, first, the alternative effects of EB (the second model), LRB (the third model) and FPB (the forth model) instead of neoprene have been evaluated and compared in three separate models and then when the deck with rigid connection is on the cap beams and abutments (the first model) have been evaluated in another model. Fig. 10 shows a view of the studied model.

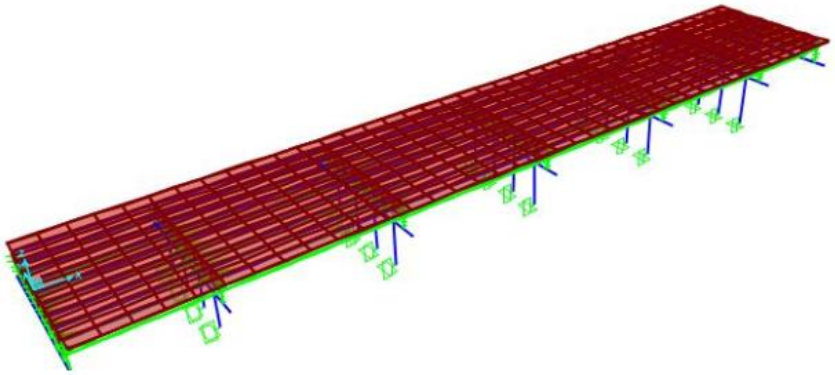

Figure 10a. A three-dimensional view of the studied model

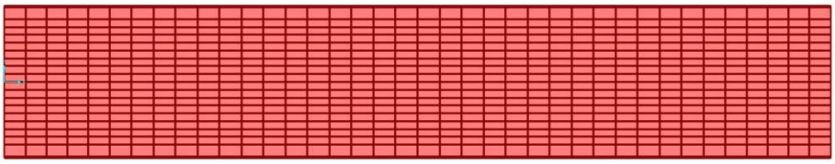

Figure 10b. A view of plan of the studied model

Figure 10. The studied model

5 EIGEN VECTOR ANALYSIS

In tables. 1 to 8, modal participating mass ratios and modal participation factors are investigated for all models. According to Tables. 1 and 2, the dominant mode in the direction y is the first mode of the structure and the dominant mode in the direction x is the fifteenth mode of the structure.

Table 1. Modal participating mass ratios for model 1

Output Case	Step Type	Step Num	Period	UX	UY	Sum UX	Sum UY
Text	Text	Unit less	Sec	Unit less	Unit less	Unit less	Unit less
MODAL	Mode	1	0.14967	2.552E-13	0.6229	2.552E-13	0.6229
MODAL	Mode	2	0.097826	4.019E-12	0.00000494	4.274E-12	0.6229
MODAL	Mode	3	0.094633	0.0001316	3.299E-15	0.0001316	0.6229
MODAL	Mode	4	0.094459	1.624E-15	0.0001457	0.0001316	0.6231
MODAL	Mode	5	0.0884	1.362E-13	0.0016	0.0001316	0.6247
MODAL	Mode	6	0.087574	0.0014	6.422E-16	0.0015	0.6247
MODAL	Mode	7	0.081984	1.866E-13	0.00005467	0.0015	0.6247
MODAL	Mode	8	0.080536	0.002	1.87E-14	0.0036	0.6247
MODAL	Mode	9	0.078159	1.751E-13	0.0022	0.0036	0.627
MODAL	Mode	10	0.078037	0.00003259	2.802E-14	0.0036	0.627
MODAL	Mode	11	0.076183	0.0004202	3.885E-15	0.004	0.627
MODAL	Mode	12	0.075215	0.0014	1.687E-15	0.0054	0.627
MODAL	Mode	13	0.07153	0.0043	2.613E-14	0.0098	0.627
MODAL	Mode	14	0.068336	0.007	1.485E-12	0.0168	0.627
MODAL	Mode	15	0.066005	0.7423	1.703E-09	0.7591	0.627

Table 2. Modal participation factors for model 1

Output Case	Step Type	Step Num	Period	UX	UY	Modal Mass	Modal Stiff
Text	Text	Unit less	Sec	Tonf-cm	Tonf-cm	Tonf-cm-s2	Tonf-cm
MODAL	Mode	1	0.14967	-0.000029	47.445713	0.1	176.2332
MODAL	Mode	2	0.097826	-0.000115	-0.133604	0.1	412.5218
MODAL	Mode	3	0.094633	0.660237	0.000003452	0.1	440.8351
MODAL	Mode	4	0.094459	-0.000002319	0.725518	0.1	442.4562
MODAL	Mode	5	0.0884	0.000021	-2.409964	0.1	505.1878
MODAL	Mode	6	0.087574	2.153852	0.000001523	0.1	514.7701
MODAL	Mode	7	0.081984	-0.000025	0.444463	0.1	587.3526
MODAL	Mode	8	0.080536	-2.599875	0.000008226	0.1	608.6686
MODAL	Mode	9	0.078159	-0.000024	-2.839625	0.1	646.2551
MODAL	Mode	10	0.078037	0.328541	0.00001	0.1	648.269
MODAL	Mode	11	0.076183	-1.179793	0.000003748	0.1	680.2127
MODAL	Mode	12	0.075215	2.166207	-0.000002476	0.1	697.8342
MODAL	Mode	13	0.07153	-3.7931	-0.000009718	0.1	771.5948
MODAL	Mode	14	0.068336	-4.826034	0.000073	0.1	845.3889
MODAL	Mode	15	0.066005	49.585043	-0.002481	0.1	906.1601

By examining the shapes of the dominant modes of the structure according to Figs. 11 and 12, it is clear that in the first mode, the deck and columns are deformed simultaneously, and in the fifteenth mode, the deformations of the deck and columns are intensified.

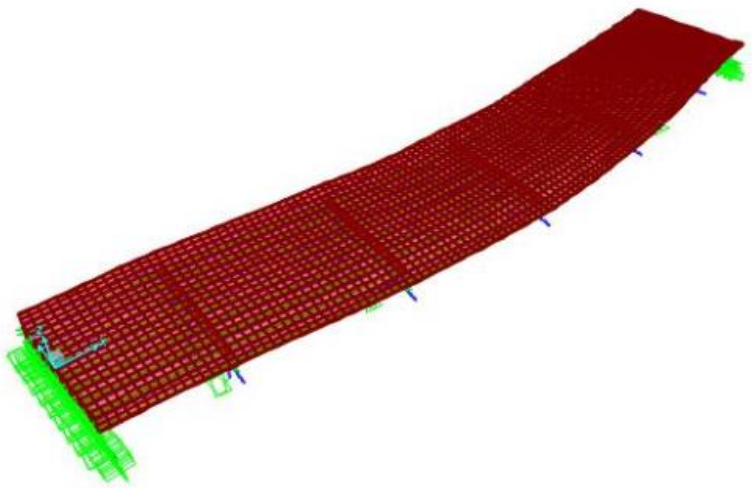

Figure 11a. A three-dimensional view of the first mode of the first model

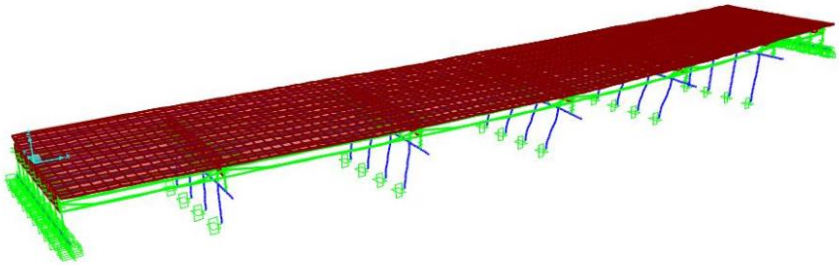

Figure 11b. An another three-dimensional view of the first mode of the first model

Figure 11c. A view of plan of the first mode of the first model

Figure 11. The first mode of the first model

Figure 12a. A three-dimensional view of the fifteenth mode of the first model

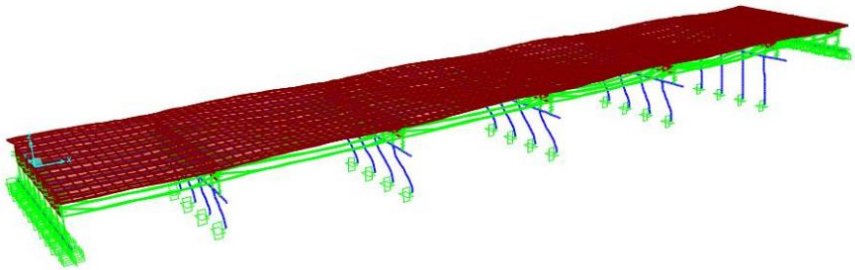

Figure 12b. An another three-dimensional view of the fifteenth mode of the first model

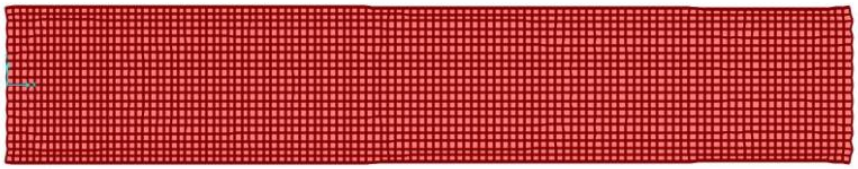

Figure 12c. A view of plan of the fifteenth mode of the first model

Figure 12. The fifteenth mode of the first model

According to Tables. 3 and 8, the dominant mode in the direction x is the first mode of the structure and the dominant mode in the direction y is the second mode of the structure for second, third and fourth models, respectively.

Table 3. Modal participating mass ratios for model 2

Output Case	Step Type	Step Num	Period	UX	UY	Sum UX	Sum UY
Text	Text	Unit less	Sec	Unit less	Unit less	Unit less	Unit less
MODAL	Mode	1	0.964956	0.7658	4.765E-20	0.7658	4.765E-20
MODAL	Mode	2	0.931987	1.832E-20	0.6774	0.7658	0.6774

Table 4. Modal Participation Factors for model 2

Output Case	Step Type	Step Num	Period	UX	UY	Modal Mass	Modal Stiff
Text	Text	Unit less	Sec	Tonf-cm	Tonf-cm	Tonf-cm-s2	Tonf-cm
MODAL	Mode	1	0.964956	50.364892	-1.312E-08	0.1	4.2398
MODAL	Mode	2	0.931987	7.789E-09	49.477104	0.1	4.5451

Table 5. Modal participating mass ratios for model 3

Output Case	Step Type	Step Num	Period	UX	UY	Sum UX	Sum UY
Text	Text	Unit less	Sec	Unit less	Unit less	Unit less	Unit less
MODAL	Mode	1	1.394352	0.7489	1.843E-18	0.7489	1.843E-18
MODAL	Mode	2	1.368985	2.162E-18	0.6729	0.7489	0.6729

Table 6. Modal participation factors for model 3

Output Case	Step Type	Step Num	Period	UX	UY	Modal Mass	Modal Stiff
Text	Text	Unit less	Sec	Tonf-cm	Tonf-cm	Tonf-cm-s2	Tonf-cm
MODAL	Mode	1	1.394352	49.804711	8.161E-08	0.1	2.0306
MODAL	Mode	2	1.368985	8.463E-08	-49.313276	0.1	2.1065

Table 7. Modal participating mass ratios for model 4

Output Case	Step Type	Step Num	Period	UX	UY	SumUX	SumUY
Text	Text	Unitless	Sec	Unitless	Unitless	Unitless	Unitless
MODAL	Mode	1	1.437885	0.7478	9.442E-19	0.7478	9.442E-19
MODAL	Mode	2	1.413183	1.078E-18	0.6727	0.7478	0.6727

Table 8. Modal participation factors for model 4

Output Case	Step Type	Step Num	Period	UX	UY	Modal Mass	Modal Stiff
Text	Text	Unit less	Sec	Tonf-cm	Tonf-cm	Tonf-cm-s2	Tonf-cm
MODAL	Mode	1	1.437885	49.768281	5.841E-08	0.1	1.9095
MODAL	Mode	2	1.413183	5.975E-08	-49.303663	0.1	1.9768

In Figs. 13 to 18, the shape of the dominant modes of the second to fourth models is shown. According to tables. 3 to 8, the first and second modes in the second to fourth models are the dominant modes in the directions x and y, respectively, which by examining modes shapes of them according to Figs. 13 to 18, it is clear that in these modes the deck slides on the seismic bearings without having the deformation.

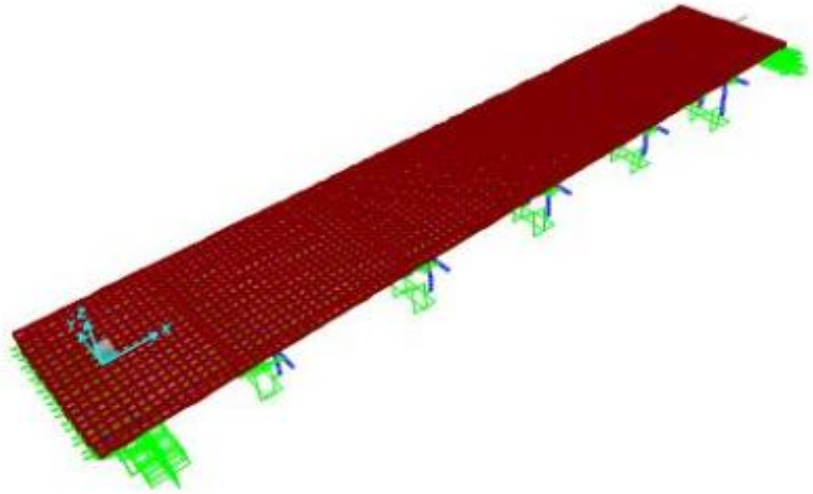

Figure 13a. A three-dimensional view of the first mode of the second model

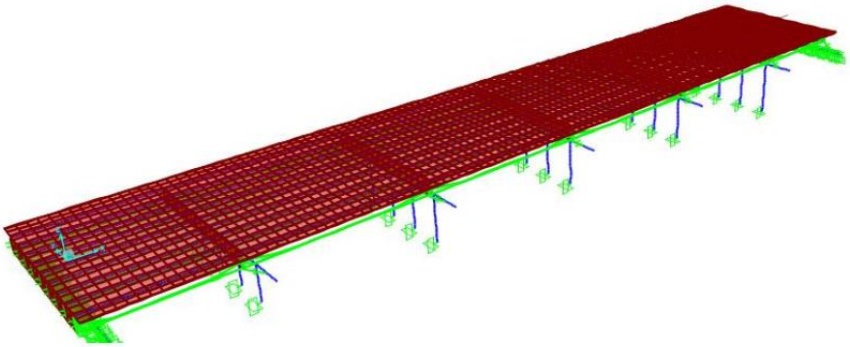

Figure 13b. An another three-dimensional view of the first mode of the second model

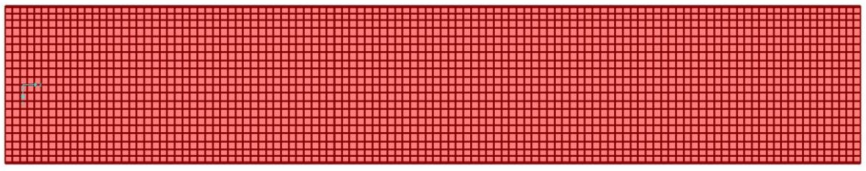

Figure 13c. A view of plan of the first mode of the second model

Figure 13. The first mode of the second model

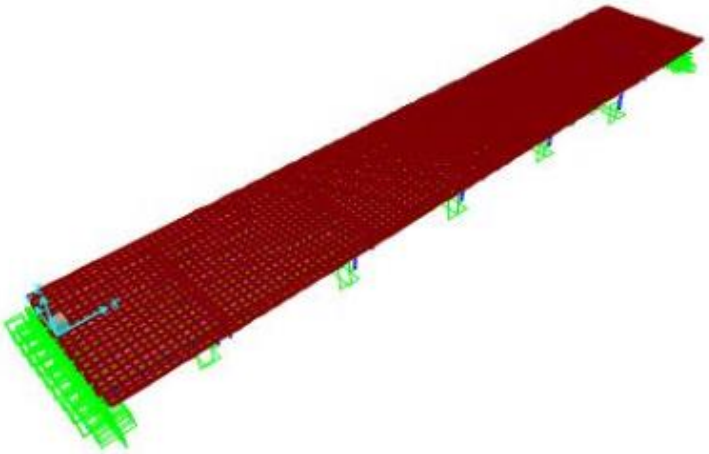

Figure 14a. A three-dimensional view of the second mode of the second model

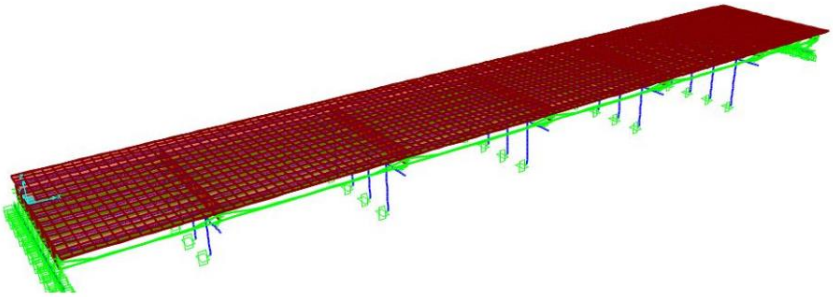

Figure 14b. An another three-dimensional view of the second mode of the second model

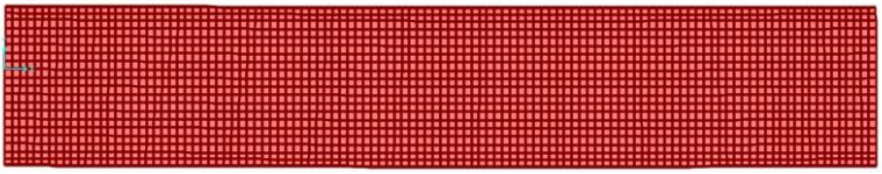

Figure 14c. A view of plan of the second mode of the second model

Figure 14. The second mode of the second model

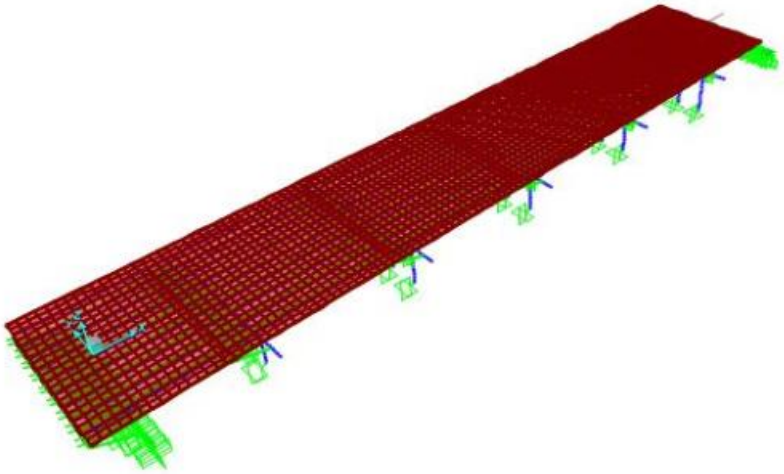

Figure 15a. A three-dimensional view of the first mode of the third model

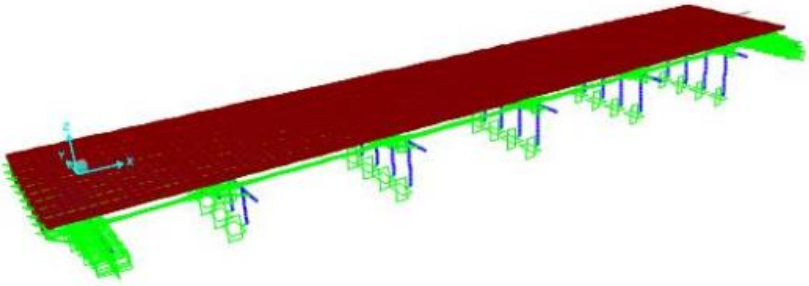

Figure 15b. An another three-dimensional view of the first mode of the third model

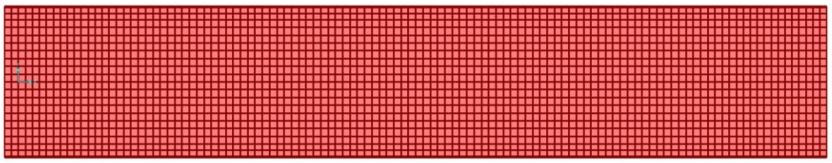

Figure 15c. A view of plan of the first mode of the third model

Figure 15. The first mode of the third model

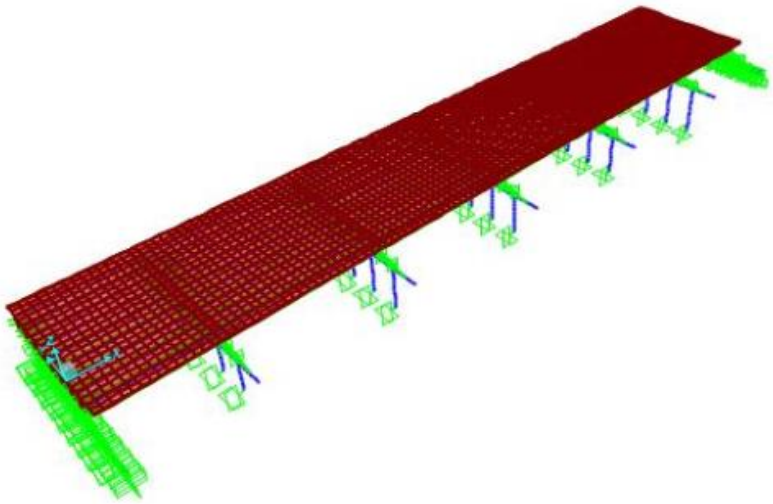

Figure 16a. A three-dimensional view of the second mode of the third model

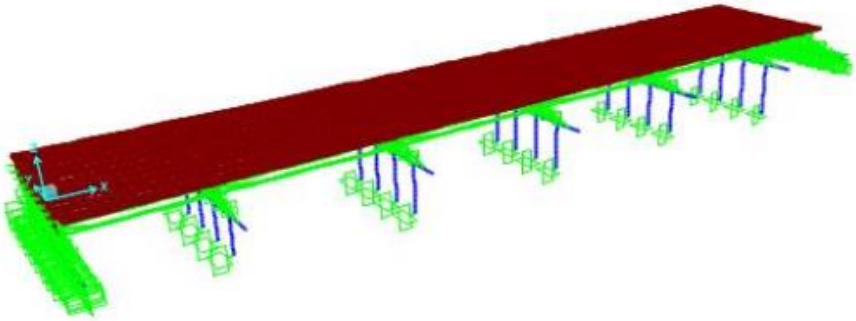

Figure 16b. An another three-dimensional view of the second mode of the third model

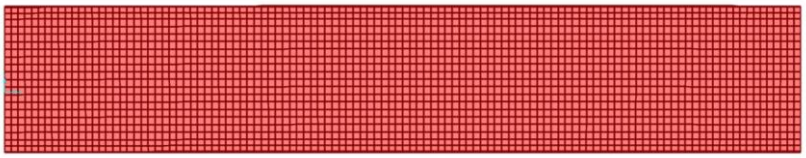

Figure 16c. A view of plan of the second mode of the third model

Figure 16. The second mode of the third model

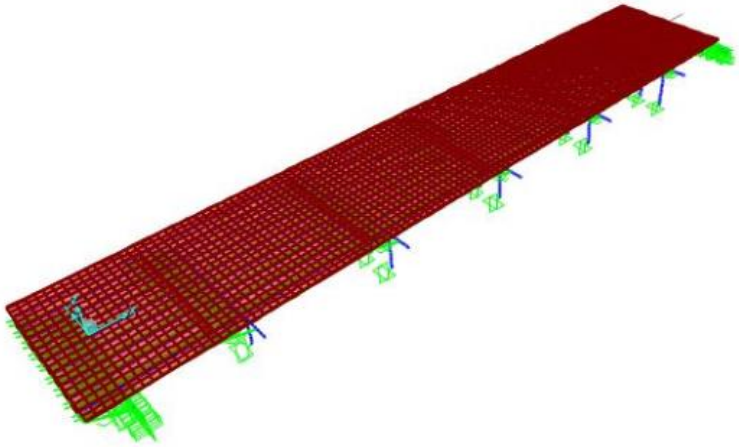

Figure 17a. A three-dimensional view of the first mode of the fourth model

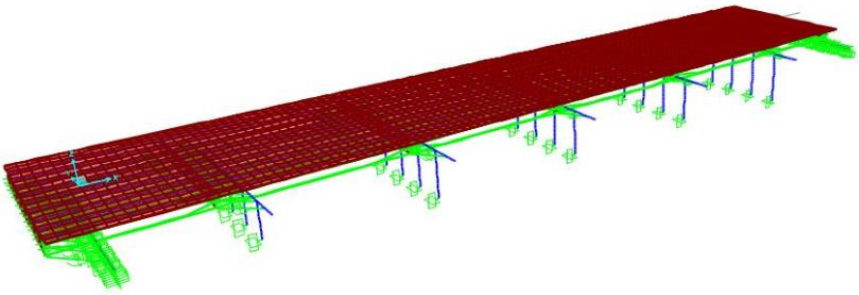

Figure 17b. An another three-dimensional view of the first mode of the fourth model

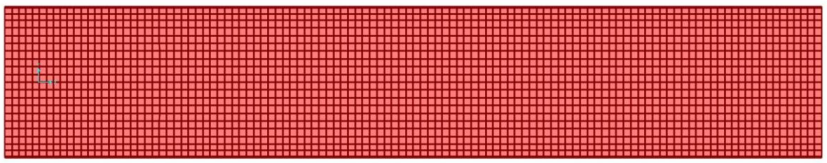

Figure 17c. A view of plan of the first mode of the fourth model

Figure 17. The first mode of the fourth model

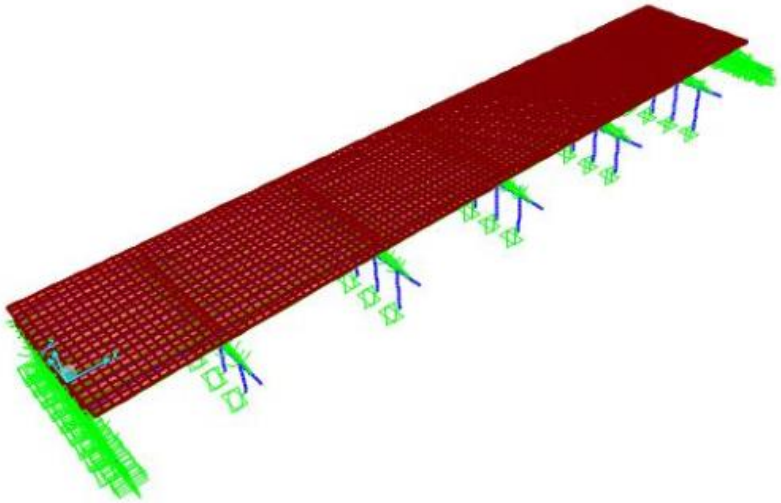

Figure 18a. A three-dimensional view of the second mode of the fourth model

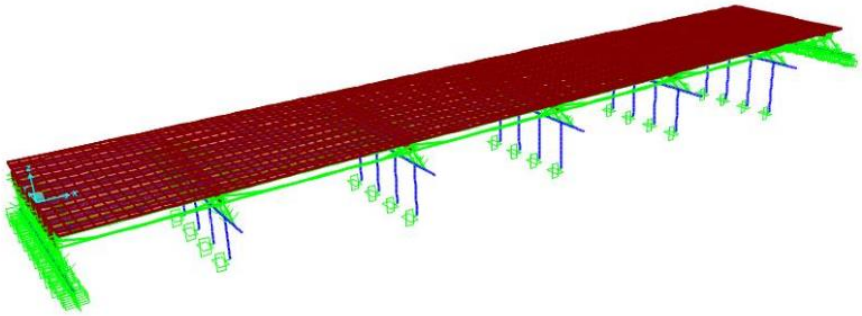

Figure 18b. An another three-dimensional view of the second mode of the fourth model

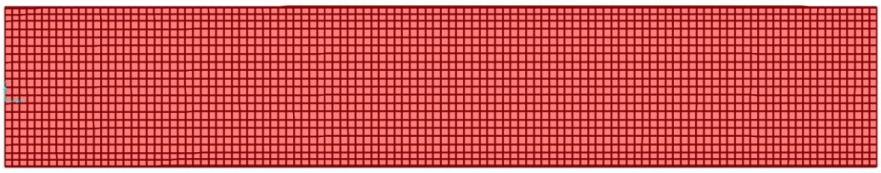

Figure 18c. A view of plan of the second mode of the fourth model

Figure 18. The second mode of the fourth model

By examining the modal participating mass ratios and modal participation factors of different models according to tables 1 to 8 and the shapes of their modes according to Figs. 11 to 18, it is clear that in the first model, most of the energy leads to vibrations is dissipated in the first and fifteenth modes, in which the structures have complex distortions in these modes, but most of the energy leads

to vibrations in models that use seismic bearings is dissipated in their first and second modes, which are the dominant modes and in these modes, structures do not have complex deformations.

By investigating the periods of the first modes of the studied models according to Fig. 19, it is clear that by using EB, LRB and FPB compared to the first model, the stiffness of the structure decreases and its period increases several times, so that the period of the first mode of the first model is 0.14 seconds, which increases to 0.96, 1.39 and 1.43 second using EB, LRB and FPB, respectively.

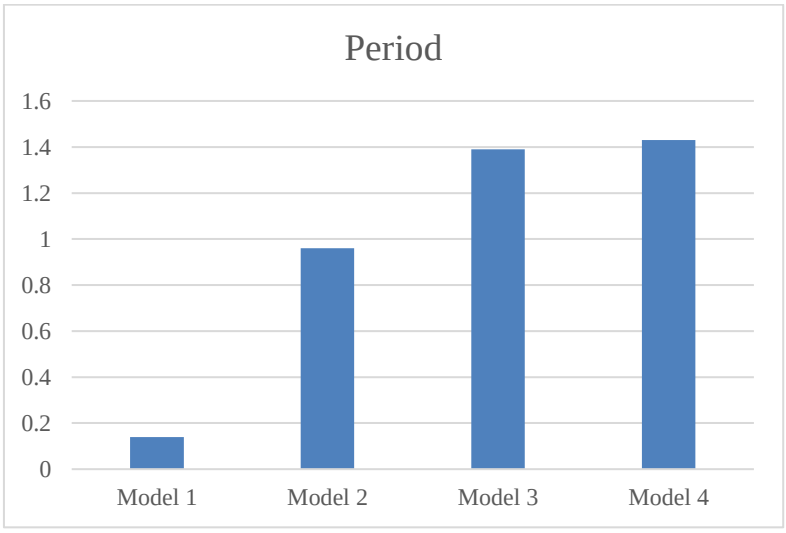

Figure 19. The period of the studied models

6 THE CHARACTERISTICS OF SELECTED EARTHQUAKES

The selected accelerograms were related to the Chi-Chi, Landers, Loma Prieta, Northridge, Parkfield, San Fernando, and Tabas earthquakes, which were selected and scaled according to Iranian Standard No. 2800 (Mansouri, 2017). Characteristics, including the magnitude, the distance from the fault, and the mechanism of the site, were considered in the selection of the accelerograms.

These accelerograms were related to the stations registered at the distance of 20 to 60 kilometers from the fault with no near-fault earthquakes characteristics, such as forward directivity and fling-step. Furthermore, the magnitude of all the selected earthquakes was between 6.5 and 7.5 Richter. The spectrum of each earthquake is shown in Fig. 20, and the spectrum of Iranian Standard No. 2800 and spectrum of earthquakes' mean is indicated in Fig. 21.

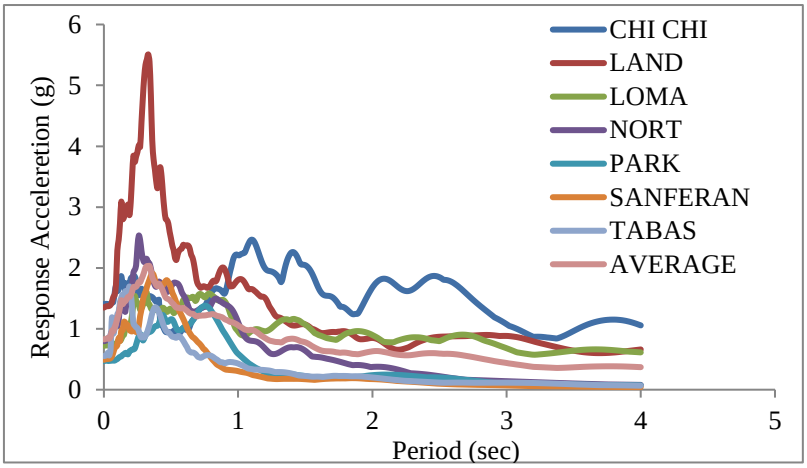

Figure 20. The spectrums of selected earthquakes

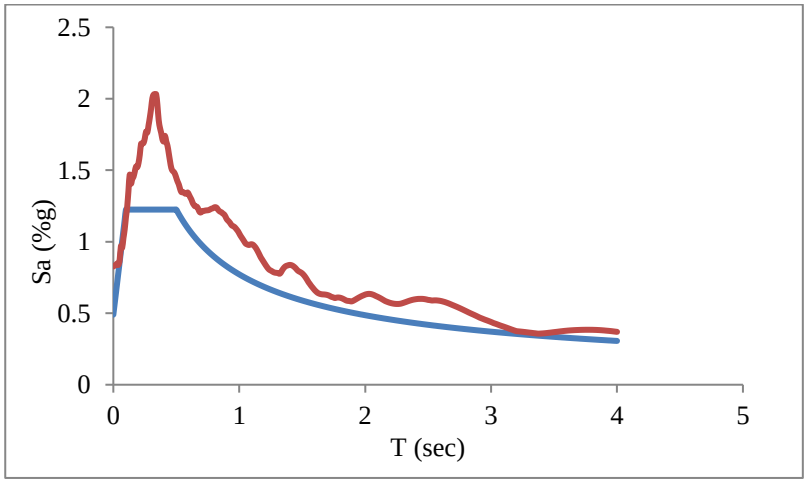

Figure 21. The comparison of the spectrum of Iranian Standard No. 2800 with earthquakes' mean spectrum.

7 NONLINEAR TIME HISTORY ANALYSIS

The seismic response of the studied bridge was investigated subjected to two components of horizontal orthogonal of Tabas earthquake. According to Fig. 22, point Deck is at the middle of the deck, and point Cap beam is in the middle of the cap beam. The unit system of all graphs and tables is in Ton-cm.

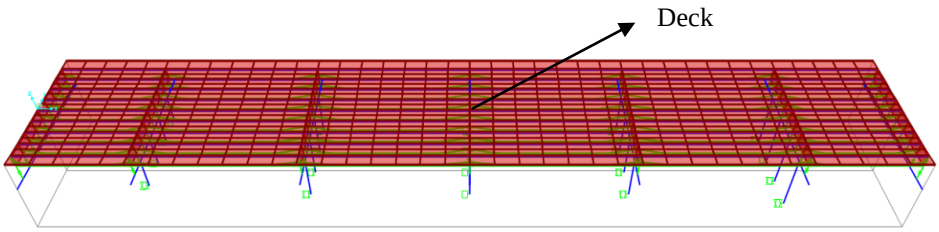

Figure 22a. Point Deck

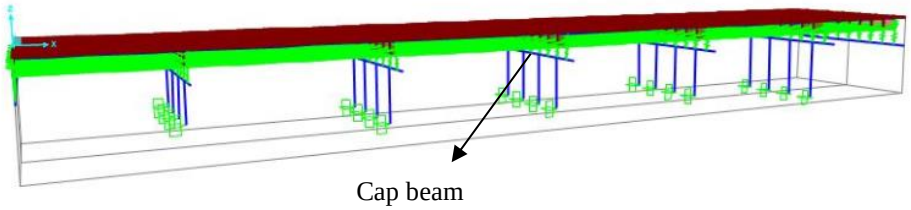

Figure 22b. Point Cap beam

Figure 22. The studied points

7.1 Results of lateral displacement

In Figs. 23 to 30, the results of the horizontal displacements of points Deck and Cap beam are presented.

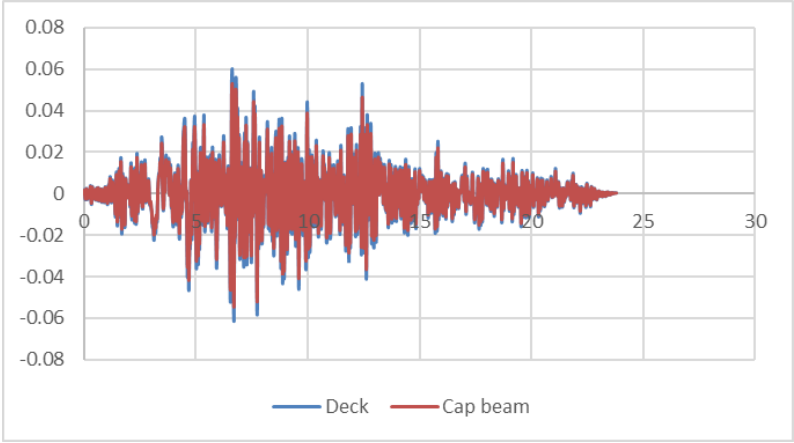

Figure 23. The lateral displacement of points Deck and Cap beam in longitudinal direction (X) in model 1.

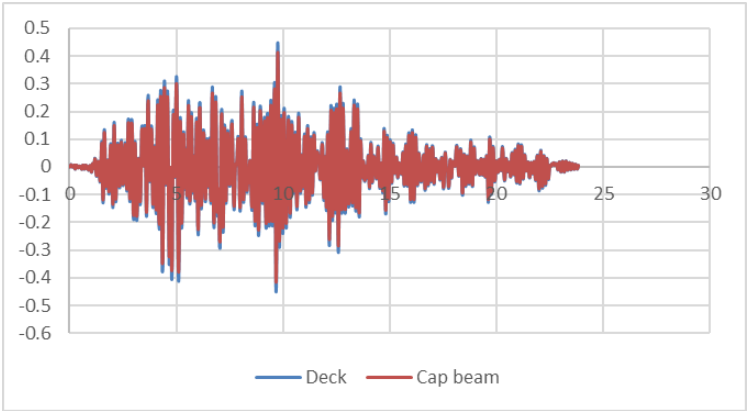

Figure 24. The lateral displacement of points Deck and Cap beam in transverse direction (Y) in model 1.

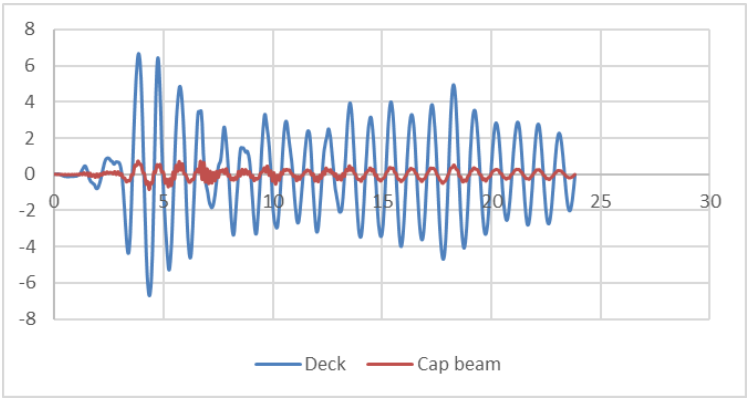

Figure 25. The lateral displacement of points Deck and Cap beam in longitudinal direction (X) in model 2.

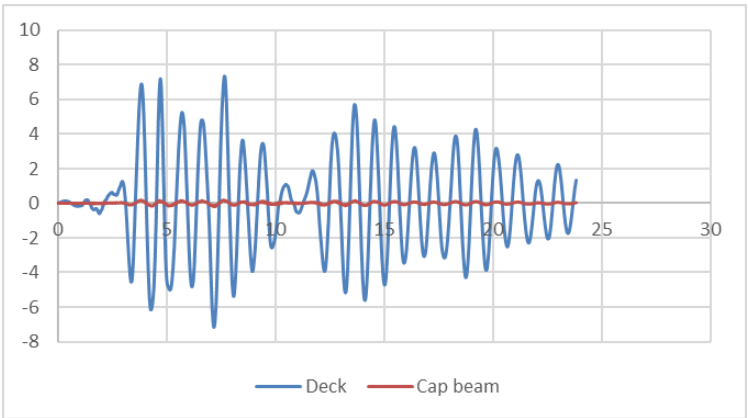

Figure 26. The lateral displacement of points Deck and Cap beam in transverse direction (Y) in model 2.

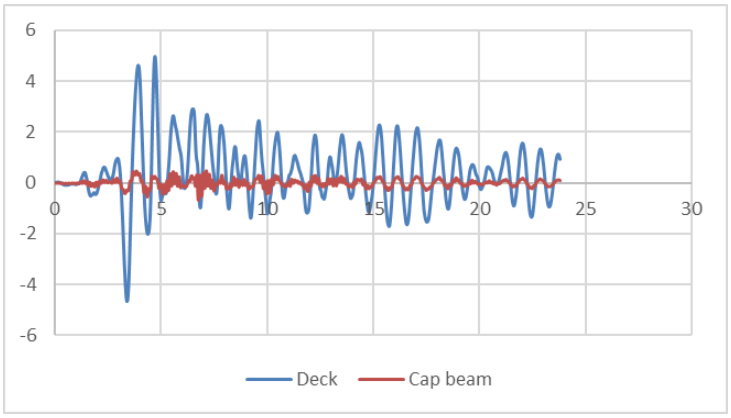

Figure 27. The lateral displacement of points Deck and Cap beam in longitudinal direction (X) in model 3.

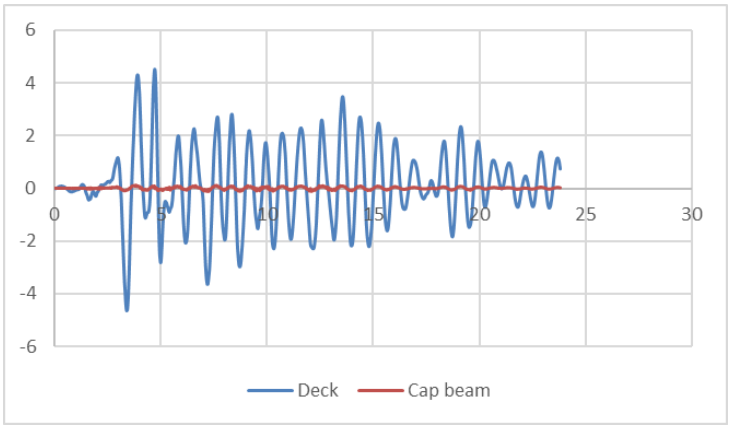

Figure 28. The lateral displacement of points Deck and Cap beam in transverse direction (Y) in model 3.

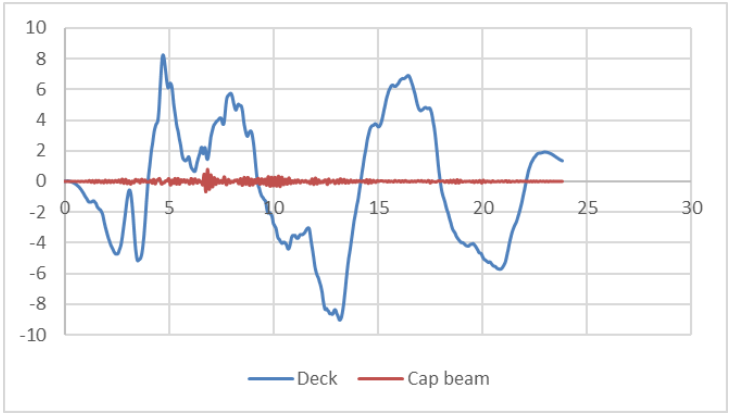

Figure 29. The lateral displacement of points Deck and Cap beam in longitudinal direction (X) in model 4.

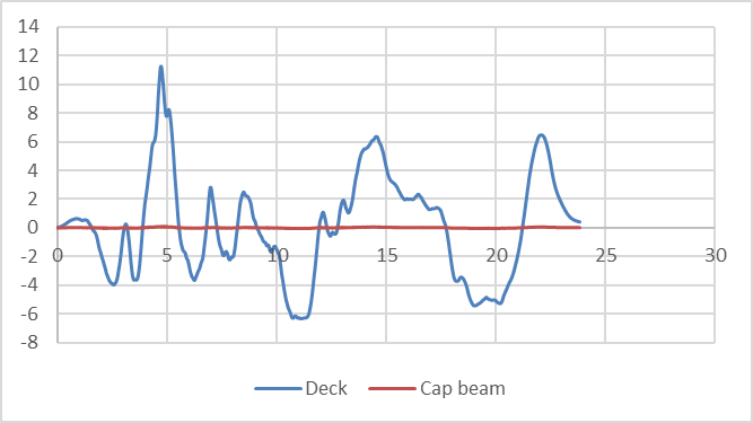

Figure 30. The lateral displacement of points Deck and Cap beam in transverse direction (Y) in model 4.

By examining Figs. 23 and 24, it is clear that in the first model, due to the earthquake, the horizontal displacement of the studied points in the longitudinal and transverse directions is equal to each other and is very small.

According to Figs. 25 to 30 in the second, third and fourth models, the deck slips due to the earthquake on the seismic bearings and the displacement of the cap beams is much less than the deck and is almost zero. Sliding deck under the effect of earthquake on the cap beams and abutments in the second to fourth models compared to the integrated behavior of the deck with the cap beams and abutments in the first model helps to prevent common seismic damages at the connection between deck with the cap beams and abutments.

The maximum horizontal displacement of the cap beams in the second, third and fourth models is approximately equal to zero, and the maximum displacement of the deck in the longitudinal and transverse directions for the second model is 6.7 and 7.34cm, in the third model is equal to 4.9 and 4.6cm and in the fourth model is equal to 9 and 11.3cm, respectively.

7.2 Results of input energy and kinetic energy

Figs. 31 to 38 show the Input energy and Kinetic energy values for different models.

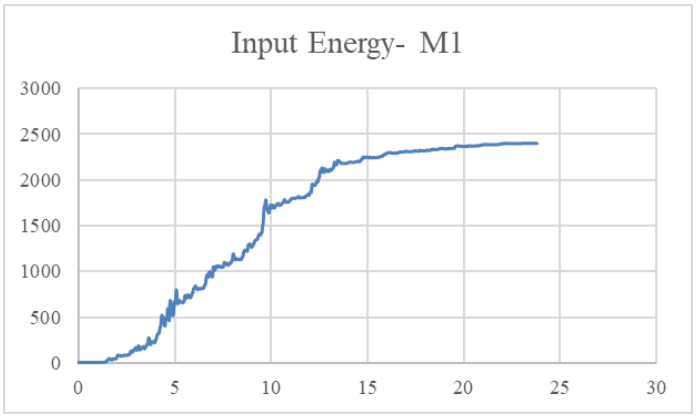

Figure 31. The results of Input energy of the bridge under the influence of Tabas earthquake for model 1.

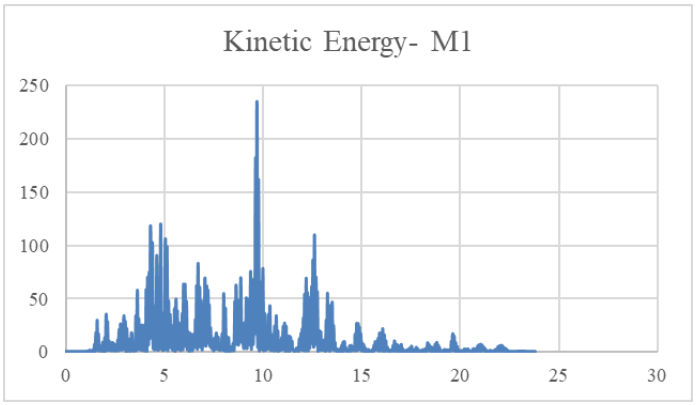

Figure 32. The results of Kinetic energy of the bridge under the influence of Tabas earthquake for model 1.

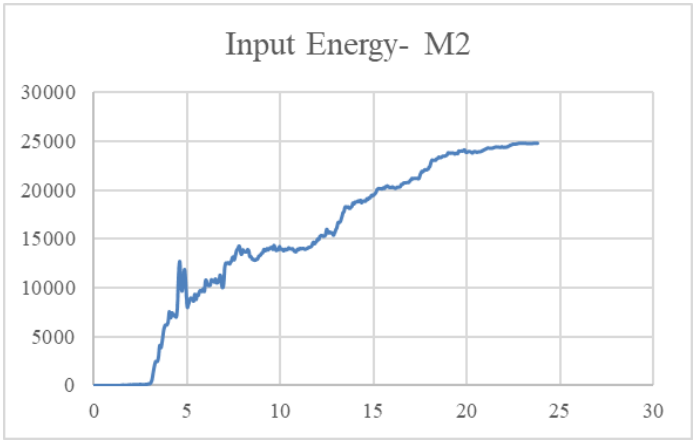

Figure 33. The results of Input energy of the bridge under the influence of Tabas earthquake for model 2.

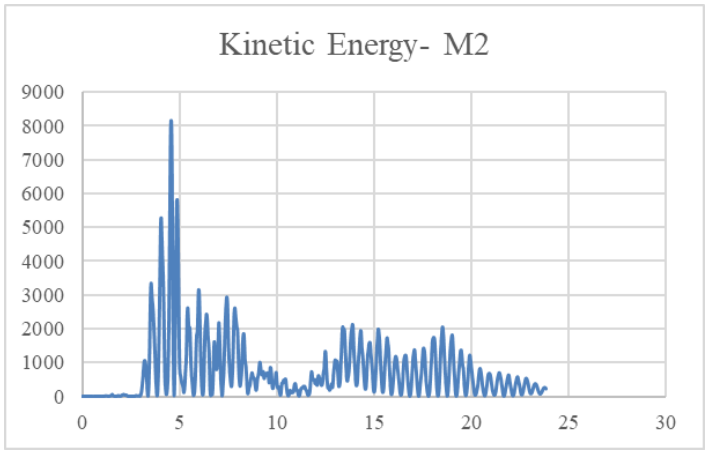

Figure 34. The results of Kinetic energy of the bridge under the influence of Tabas earthquake for model 2.

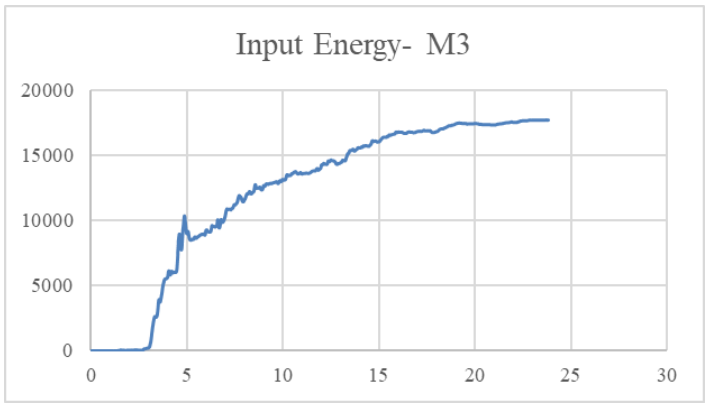

Figure 35. The results of Input energy of the bridge under the influence of Tabas earthquake for model 3.

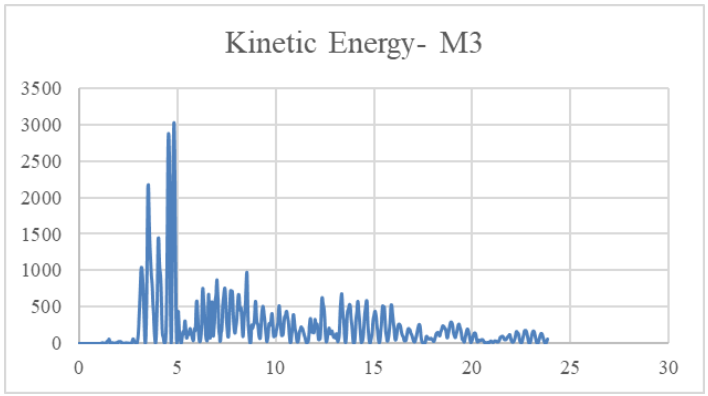

Figure 36. The results of Kinetic energy of the bridge under the influence of Tabas earthquake for model 3.

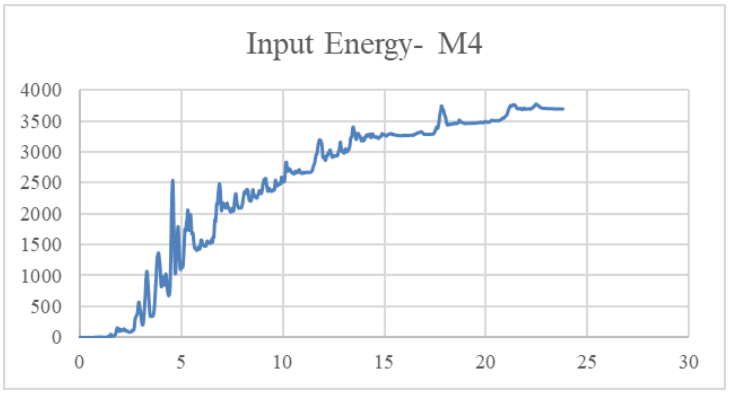

Figure 37. The results of Input energy of the bridge under the influence of Tabas earthquake for model 4.

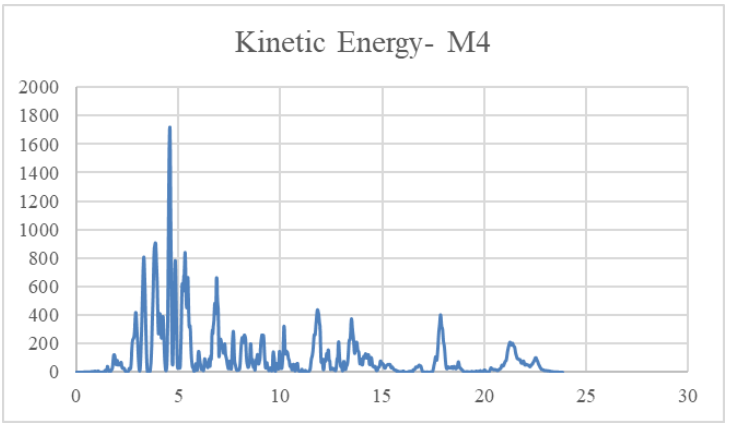

Figure 38. The results of Kinetic energy of the bridge under the influence of Tabas earthquake for model 4.

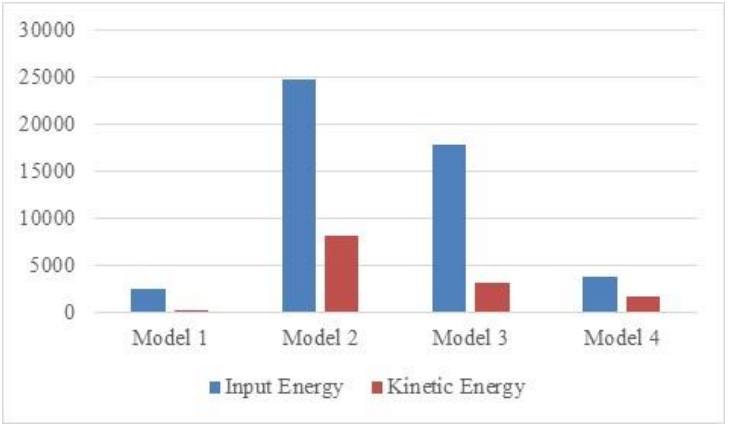

Figure 39. Input energy and Kinetic energy results for the studied models.

Fig. 39 shows the Input energy and Kinetic energy values for different models. It is clear that in the first model, the bridge has significant stiffness, for this model, the values of Input energy and Kinetic energy are not significant for the structure. By using seismic bearings, the stiffness of the bridge is reduced and as a result, the Input energy and Kinetic energy values increase significantly for the second to fourth models compared to the first model.

7.3 Results of base shear

According to Fig. 40, the results of studies indicated that the application of the using seismic bearings could affect the base shear of the studied bridge considerably than its non-application. Fig. 40 shows the result of base shear in longitudinal (X) and transversal (Y) directions for all models.

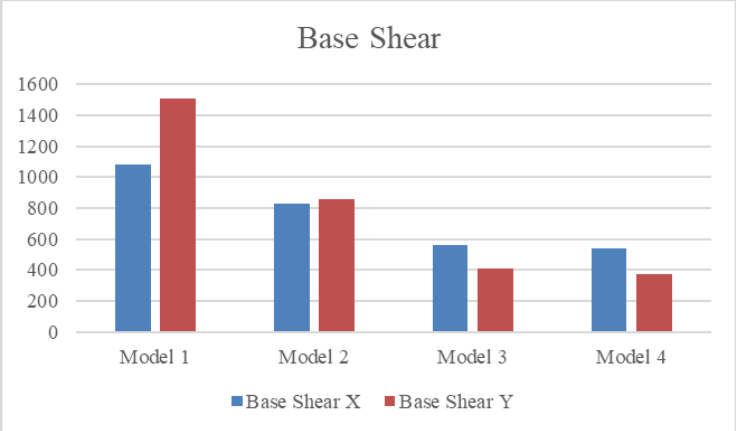

Figure 40. The results of base shear of the bridge in longitudinal (X) and transversal (Y) directions under the influence of Tabas earthquake

According to Fig. 40, the base shear for the first model in the directions x and y is equal to 1081 and 1505 tons, respectively. In the second model, by using elastomeric bearing, the base shear of the bridge is reduced and got to 825 and 853.6 tons, respectively. In the third model, with using LRB in the bridge, the base shear of the structure is reduced and reached 563.7 and 405.3 tons, based on order. The base shear in the fourth model, which uses FPB in the bridge, in the directions x and y is equal to 541.1 and 370.2, respectively.

8 CONCLUSION

In the isolated bridges, the first and second modes of the structure are the dominant modes, in which the columns are without deformation and only the deck slides on the seismic bearings, but in the first model (integrated bridge), the first and fifteenth modes are the dominant modes, in which the decks and columns undergo complex deformations.

By examining modal participation factors and modal participating mass ratios for the studied structures and the shape of their modes, it is clear that by using seismic bearings, complex deformations of decks and columns can be prevented compared to the first model (integrated bridge) and most of the energy due to vibrations in the isolated bridges compared to the integrated bridges is dissipated in modes (dominant modes) in which the structure has very simple deformations.

Separating the bridge deck from the cap beams and abutments and placing seismic bearings in this place (second, third and fourth models) compared to the rigid connection of the deck to the cap beams and abutments (first model) reduces the stiffness of the structure and increases its period. The period of the first mode of the first model is 0.14 seconds, which increases to 0.96, 1.39 and 1.43 seconds using EB, LRB and FPB, respectively.

By examining the horizontal displacement of the deck and cap beams, it is clear that in the first model, where the deck is rigidly connected to the cap beams and abutments, the horizontal displacement of the deck and cap beams is equal and its values is very small. This seismic behavior causes a significant seismic response of the structure, but by using seismic bearings, the deck slides on this equipment and this seismic behavior causes a significant reduction of the seismic response of the structure.

It is clear that in the first model, due to the earthquake, the horizontal displacement of the studied points in the longitudinal and transverse directions is equal to each other and is very small. In the second, third and fourth models, the deck slips due to the earthquake on the seismic bearings and the displacement of the cap beams is much less than the deck and is almost zero. The maximum displacement of the deck in the longitudinal and transverse directions for the second model is 6.7 and 7.34cm, in the third model is equal to 4.9 and 4.6cm and in the fourth model is equal to 9 and 11.3cm, respectively.

In the first model, the bridge has significant stiffness that the values of Input energy and Kinetic energy are not significant for the bridge. By using seismic bearings, the stiffness of the bridge is reduced and as a result, the Input and Kinetic energy values increase significantly for the second to fourth models compared to the first model.

By examining the results of the base shear for different models, it is clear that the using seismic bearings in between the deck with cap beams and abutments compared to the case where the deck with a rigid connection is on the cap beams and abutments leads to reduce the base shear of the bridge. By comparing the results of the second, third and fourth models, it is clear that the base shear in the mode of using FPB is reduced to a greater extent than the mode of using EB and LRB. So that, the base shear for the first model in the directions x and y is equal to 1081 and 1505 tons, respectively. In the second model, by using elastomeric bearing, the base shear of the bridge is reduced and reached 825 and 853.6 tons, based on order. In the third model, by using LRB, the base shear of the structure is reduced and got to 563.7 and 405.3 tons, based on order. The base shear in the

fourth model, which uses FPB in the bridge, in the directions x and y is equal to 541.1 and 370.2, respectively.

Decreasing the stiffness of the structure and increasing its period, increasing the Input and Kinetic energy of the structure and significantly reducing the base shear of the structure indicate the seismic retrofit of the structure in the case of using seismic bearings compared to the rigid connection between the deck to cap beams and abutments.

According to the results of the present study, the best solution among the options considered for seismic retrofit of the studied bridge is to replace FPB with conventional neoprene.

REFERENCES

[1] Akogul, C., and Celik, O, C., "Effect of elastomeric bearing modeling parameters on the seismic design of RC highway bridges with precast concrete girders", *The 14th world conference on earthquake engineering*, Beijing, China, 2008.

[2] Avossa, A, M., Giacinto, D, D., Malangone, P., Rizzo, F., "Seismic retrofit of a multi-span pre-stressed concrete girder bridge with friction pendulum devices", Journal of shock and vibration, Article ID 5679480, Vol 2018.

[3] Caterino, N., Maddaloni, G., Occhiuzzi, A., "Damage analysis and seismic retrofitting of a continuous prestressed reinforced concrete bridge", Case studies in structural engineering, Vol 2, Pages 9–15, 2014.

[4] Han, K, B., Hong, S, N., Park, S, K., Seismic performance evaluation of retrofitted bridge by isolation bearings, The Baltic journal of road and bridge engineering, Volume 4, Issue 3, Pages 134–142, 2009.

[5] Jabbareh Asl, M., Rahman, M., Karbakhsh, A., Numerical Analysis of Seismic Elastomeric Isolation Bearing in the Base-Isolated Buildings, Open Journal of Earthquake Research, Vol. 3, 2014.

[6] Ju, S, H., Yuantien, C, C., Hsieh, W, K., "Study of lead rubber bearings for vibration reduction in high-tech factories", Journal of applied sciences, Vol 10, No.4, 2020.

[7] Kaheh, P., "Application study of the elastomeric bearing with performance ability to vibration Isolator in reduce of force demand due of earthquake and case study", Department of civil engineering, *«M.Sc» Thesis on structural engineering*, University of Tehran, Tehran, Iran, 2011. (In Persian).

[8] Li, B., Wang, B., Wang, S., Xiao Wu, X., "Energy response analysis of continuous beam bridges with friction pendulum bearing by multi-hazard source excitations", Journal of shock and vibration, Article ID 3724835, Vol 2020.

[9] Li, X., Shi, Y., "Seismic design of bridges against near-fault ground motions using combined seismic isolation and restraining systems of LRBs and CDRs", Journal of shock and vibration, Vol 2019.

[10] Ma, X, T., Bao, C., Doh, S, I., Lu, H., Zhang, L, X., Ma, Z, W., He, Y, T., Dynamic response analysis of story-adding structure with isolation technique subjected to near-fault pulse-like ground motions, Physics and Chemistry of the Earth, Parts A/B/C, 2020.

[11] Ma, X, T., Bao, C., Doh, S, I., Lu, H., Zhang., L, X., Ma, Z, W., He, Y, T., "Dynamic response analysis of story-adding structure with isolation technique subjected to near-fault pulse-like ground motions", Journal of physics and chemistry of the earth, Vol 121, 2021.

[12] Mansouri, S., Mansouri S., Nazari, A., *"*The investigation of different methods of repairing and seismic retrofitting railway bridges by case study*", International Conference on Engineering, Arts and the Environment*, International Center of Academic Communication (ICOAC), University of Szczecin, 2014. (in Persian).

[13] Mansouri, S., Mansouri S., Nazari, A., Amraei, Mehdi., "The investigation of common seismic damages of reinforced concrete bridges and the presentation of the strategies for reducing distortion of deformation modes of bridges using Eigen vector analysis", *2nd International Congress on Structure, Architecture and Urban Development*, Tabriz, Iran, 2014. (in Persian).
[14] Mansouri, S., Mansouri S., Nazari, A., "The investigation of the strategies to increase the number of stories in the existing buildings using energy dissipation devices", *2nd International Congress on Structure, Architecture and Urban Development*, Tabriz, Iran, 2014. (in Persian).
[15] Mansouri, S., Mansouri, S., Ghanbari, F., "The study of different codes in terms of application of vertical component of earthquake in the estimation the seismic response of structures through case studies", *2nd International Congress on Structure, Architecture and Urban Development*, Tabriz, Iran, 2014. (in Persian).
[16] Mansouri, S., Mansouri S., Nazari, A., Derikvand, Z., "The comprehensive investigation of seismic retrofit of RC high-rise buildings using friction pendulum bearings through nonlinear time history analysis", *1st national Conference on Architecture, civil and Urban Development*, Tabriz, Iran, 2014. (in Persian).
[17] Mansouri, S., Mansouri S., Nazari, A., Mansouri, N., "The investigation of the effects of using lead-rubber bearings, friction pendulum bearings and tuned mass dampers in seismic retrofitting buildings", *8th international Conference on New Advances in Engineering Sciences*, Tonekabon, Mazandaran, Iran, 2014. (in Persian).
[18] Mansouri, S., Mansouri S., Nazari, A., "The investigation of the effects of the excitations of two-components and three-components of the earthquake on the response of irregular bridges according to standard loads for bridges (Iranian code No. 139) and road and railway bridges seismic resistant design code (Iranian code No. 463) through case studies", *7th International Conferences of Seismology and Earthquake Engineering (SEE7)*, International Institute of Earthquake Engineering and Seismology (IIEES), 2015. (in Persian).
[19] [19] Mansouri, S., Mansouri S., "The seismic retrofit of an existing bridge using energy dissipation equipment and nonlinear time history analysis", *4th international conference of bridges*, Amirkabir University, Tehran, Iran. 2015. (in Persian).
[20] Mansouri, S., "The seismic retrofit of an existing bridge using energy dissipation equipment", Research bulletin of seismology and earthquake engineering, IIEES, Vol 19, Issue 4, Pages 19-32, 2016. (in Persian)
[21] Mansouri, S., and Nazari, A., "The effects of using different seismic bearing on the behavior and seismic response of high-rise building", Civil engineering journal, Vol 3, Issue 3, Pages 160-171, 2017.
[22] Mansouri, S., "The assessment of the equivalent static analysis method of AASHTO code in the estimation of seismic response of the bridges equipped with energy dissipation equipment", Research bulletin of seismology and earthquake engineering, (IIEES), Vol 20, Issue 3, Pages 71-86, 2017. (in Persian)
[23] Mansouri, S., "Interpretation of "Iranian code of practice for seismic resistant design of building (standard No. 2800, 4th edition)"", Published by Simaye Danesh, Tehran, Iran, 2017.
[24] Mansouri, S., "The investigation of the effects of vertical earthquake component on seismic response of skewed reinforced concrete bridges", International journal of bridge engineering, Vol 8, Issue 1, Pages 35-52, 2020.
[25] Mansouri, S., "The presentation of a flowchart to select near and far-fault earthquakes for seismic design of bridges and buildings based on defensible engineering judgment", International journal of bridge engineering, Vol 9, Issue 1, Pages 35-48, 2021.
[26] Okamura, S., Fujita, S., Motion analysis of pendulum type isolation systems during earthquakes (probabilistic study of isolation performance of base isolated structure considering characteristic Dispersion of Pendulum Type Isolation Systems), Journal of Pressure Vessel Technology, Vol. 129, Pages 507- 515, 2007.
[27] Parvari, A., Hasanvand, R., Mansouri, S., "The investigation of the effects of using rocking systems on the seismic retrofit of high-rise steel building", Journal of structural engineering,

Maragheh Branch, Islamic Azad University, Vol 15, Issue 2, Pages 57-71, 2018. (in Persian)
[28] Qiang, H., Xiuli, D., Jingbo, L., Zhongxian, L., Liyun, L., Jianfeng, Z., "Seismic damage of highway bridges during the 2008 Wenchuan earthquake", Journal of earthquake engineering and engineering vibration, Vol 8, Pages 263-273, 2009.
[29] Torunbalci, N., and Ozpalanlar, G., "Earthquake response analysis of mid-story buildings isolated with various seismic isolation techniques", *The 14th world conference on earthquake engineering*, Beijing, China, 2008.
[30] Zheng, W., Wang, H., Hao, H., Bi, K., Shen, H., "Performance of bridges isolated with sliding-lead rubber bearings subjected to near-fault earthquakes", International journal of structural stability and dynamics, Vol 20, Issue 2, 2020.